J. Biochem. 128, 167–173 (2000)

Primary Structure and Autoproteolysis of Brevilysin H6 from the Venom of *Gloydius halys brevicaudus*[1]

Satoshi Fujimura, Kiyotaka Oshikawa, Shigeyuki Terada,[2] and Eiji Kimoto

Department of Chemistry, Faculty of Science, Fukuoka University, 8-19-1 Nanakuma, Jonan-ku, Fukuoka 814-0180

Received April 12, 2000; accepted May 2, 2000

The complete amino acid sequence of brevilysin H6 (H6), a zinc-protease isolated from *Gloydius halys brevicaudus* venom, was determined by a manual Edman degradation method. H6 has an amino-terminal pyroglutamic acid and consists of a total of 419 residues. An *N*-linked sugar chain is attached at Asn-181. The molecule is composed of three domains (metalloprotease, disintegrin-like and cysteine-rich domains), as commonly found in other high molecular mass metalloproteases from snake venoms. In the absence of calcium ions, H6 is autocatalytically degraded with a half-life of 47 min to give 29 and 45 kDa fragments, which correspond to residues 208–419 and 99–419 of H6, respectively. Thus, the autoproteolysis seemed to start from the cleavage of either the Leu^{98}-Leu^{99} or Asp^{207}-Ile^{208} bond. Calcium ions suppressed both the formation of the 45 kDa fragment and the rate of autoproteolysis. Calcium ions also contributed to the stability of H6 against pH, heating, urea and cysteine. More than twenty-five peptide bonds adjacent to hydrophobic residues in the metalloprotease domain were progressively cleaved during the autoproteolysis.

Key words: amino acid sequence, autoproteolysis, calcium ion, *Gloydius halys brevicaudus*, metalloprotease.

Snake venom metalloproteases and mammalian reproductive proteins belong to the reprolysin subfamily among several zinc-containing metalloproteases. They are characterized by the presence of a conservative zinc chelating sequence, HEXXH, as an essential part for the proteolytic activity (*1*). The different molecular sizes of reprolysins reflect the numbers of domains: metalloprotease, disintegrin-like, and Cys-rich domains (*2*). According to Hite *et al.* (*3*), venom reprolysins are divided into four classes (P-I to P-IV) based on the domain structure of the proteins and genes. The P-I class comprises a low molecular mass metalloprotease that is composed solely of a metalloprotease domain. The intermediate type metalloproteases (class P-II) have an additional disintegrin-like domain, which is homologous to those of platelet aggregation inhibitors (disintegrins). High molecular mass proteases (class P-III) consist of the all three domains, and the P-IV class has a C-type lectin sequence at the end of the Cys-rich domain. Mammalian metalloprotease/disintegrin proteins such as fertilin (*4*) and EAP (*5*) have additional EGF-like, transmembrane, and cytoplasmic domains.

Brevilysin H6 is one of the main proteins in *G. halys brevicaudus* venom (*6*). This enzyme is a glycoprotein with a molecular mass of 60 kDa. It shows weak hemorrhagic activity (minimum hemorrhagic dose = 8.6 μg) and rapidly degrades the Aα-chain of fibrinogen. H6 is assumed to be a metalloprotease since it contains a zinc ion and is inactivated by metal chelating agents. Calcium ions enhance its proteolytic activity up to about 400%.

In a previous paper (*7*), we reported the isolation and amino acid sequence of a 29 kDa protein from the same venom. This protein (p29K) exhibits weak inhibitory activity as to human platelet aggregation. Moreover, p29K was suggested to be derived from brevilysin H6 through autocatalytic degradation. In order to confirm the structural relationship of p29K to H6 as well as to clarify the features of the autoproteolysis, we have determined the complete amino acid sequence of brevilysin H6. On the basis of the primary structure, the scissile peptide bonds during the autocatalytic digestion of H6 were determined. We also examined the effect of Ca^{2+} on the stability and autoproteolysis of the enzyme.

MATERIALS AND METHODS

Materials—Brevilysin H6 was purified from *G. halys brevicaudus* venom as described previously (*6*) except that 10 mM $CaCl_2$ was added to each solvent. Arginylendopeptidase (Arg-C) from mouse submandibular glands, pyroglutamate aminopeptidase from porcine liver, and endopeptidase Asp-N from *Pseudomonas fragi* were purchased from Takara (Kyoto). *Achromobacter lyticus* lysyl endopeptidase (Lys-C), carboxypeptidase Y from yeast, V8 protease from *Staphylococcus aureus* V8, and all other chemicals were obtained from Wako Pure Chem. (Osaka). FTC-casein was prepared according to Twining (*8*).

SDS-PAGE and Amino Acid Analysis—SDS-PAGE was carried out on a 12% gel by the method of Laemmli (*9*). The

[1] In this article, the name *Gloydius* was used instead of the old name *Agkistrodon* for Mamushi snakes.

[2] To whom correspondence should be addressed.

Abbreviations: Arg-C, arginylendopeptidase; CM, *S*-carboxymethylated; FTC-casein, fluorescein thiocarbamoyl casein; H6, brevilysin H6 from *G. halys brevicaudus* venom; Lys-C, *Achromobacter lyticus* lysyl endopeptidase; p29K, 29 kDa fragment of brevilysin H6; TFA, trifluoroacetic acid.

amino acid composition was determined with an automated amino acid analyzer (Jasco) after samples had been hydrolyzed with 0.25% phenol–2% thioglycolic acid–6 M HCl at 110°C for 20 h in evacuated and sealed tubes.

Sequence Determination—Brevilysin H6 was reduced and *S*-carboxymethylated (CM) according to Hirs (*10*). CM-protein (4 mg each) was digested at 37°C with Arg-C (E/S = 1:50) for 4 h in 50 mM phosphate buffer (pH 8.0), Lys-C (E/S = 1:100) for 6 h in 20 mM Tris-HCl (pH 9.0), or *S. aureus* V8 protease (E/S = 1:100) for 6 h in 0.1 M NH_4HCO_3. CM-protein (6 mg each) was also cleaved chemically with *o*-iodosobenzoic acid (6 mg) in 4 M guanidine-HCl–80% acetic acid–2% *p*-cresol at room temperature for 20 h or CNBr (100 equivalent) in 70% HCOOH for 24 h. Some large peptides were further digested with endopeptidase Asp-N (E/S = 1:100) in 50 mM phosphate buffer (pH 8.0) at 37°C for 6 h. Digestion with pyroglutamate aminopeptidase (0.02 U/mg substrate) was carried out in 10 mM EDTA-10 mM dithiothreitol–50 mM phosphate buffer (pH 8.0) at 37°C for 5 h. The digests were lyophilized, dissolved in 0.1% TFA, and then fractionated by reverse-phase HPLC on a TSK-gel ODS-120T column (0.46 × 25 cm, Tosoh) in 0.1% TFA with an appropriate gradient of acetonitrile.

The amino acid sequences of peptides were determined by manual Edman degradation using the 4-*N,N*-dimethylaminoazo-benzene-4′-isothiocyanate/phenylisothiocyaate double coupling method (*11*). Amino acid derivatives were identified by the HPLC method (*12*). The C-terminal sequence of H6 was determined by carboxypeptidase Y digestion as described previously (*7*).

Assay for Endopeptidase Activity—Endopeptidase activity was measured at 37°C using 1% casein in 0.2 M Tris-HCl (pH 8.5) as described by Satake *et al.* (*13*). In some experiments, 0.2% FTC-casein was used and the increase in fluorescence was measured with a FP-550A spectrofluorometer (Jasco) at 520 nm with excitation at 490 nm (*8*).

Stability of the Enzyme as to pH, Heating, and Urea—The stability of H6 was examined at various pHs in 50 mM veronal-HCl (pH 3.8–9.0) or 50 mM Gly-NaOH (pH 8–10.9). After the enzyme solutions (0.3 mg/ml) had been kept at 37°C for 1 h, the residual activity was measured as described above. Thermal stability was examined in 10 mM TES-NaOH (pH 7.0). After the enzyme solution (0.42 mg/ml) had been stood at 0–70°C for 15 min in a water bath, the residual activity was measured. The enzyme solution (0.3 mg/ml) in 50 mM TES-NaOH (pH 7.0) containing 0–4 M urea was pre-incubated at 25°C for 5 min, and then the residual activity was measured. To evaluate the effect of Ca^{2+} on the stability of the enzyme, 2–10 mM $CaCl_2$ was added to the preincubation mixture.

Autoproteolytic Digestion of H6—H6 (1.0 mg/ml) was dissolved in 50 mM Tris-HCl (pH 8.5) or 20 mM $CaCl_2$–50 mM Tris-HCl (pH 8.5), and then incubated at 37°C for 6 and 24 h. Forty-five microliters of the reaction mixture was mixed with 15 μl of 4% SDS–50% glycerin–10% 2-mercaptoethanol–25 mM Tris-HCl (pH 6.8), and then subjected to SDS-PAGE as described above.

For isolation of the fragment peptides, H6 (5 mg) was dissolved in 0.5 ml of 50 mM Tris-HCl (pH 8.5) and then incubated at 37°C. Large fragments were isolated after 24 h by ion-exchange HPLC on a column of TSK gel DEAE-5PW (0.75 × 7.5 cm, Tosoh) with a gradient of 0.1 to 0.4 M NaCl in 1 mM $CaCl_2$–20 mM Tris-HCl (pH 8.0). Small peptide fragments were obtained after 60 h by reverse-phase HPLC on a Biofine RPC SC-18 column (0.46 × 25 cm, Jasco) with a gradient of acetonitrile in 0.1% TFA.

For kinetic experiments on autoproteolysis, H6 (0.8 μM) in 50 mM Tris-HCl (pH 8.5) containing 0.1 mM L-cysteine, 1 mM $CaCl_2$, or 10 mM $CaCl_2$ was incubated at 37°C for 5 min to 8 h. The reaction was stopped by mixing aliquots (100 μl) with 25 μl of 100 mM EDTA and then 50 μl aliquots of the mixtures were subjected to HPLC on a μBondasphere C8-300A column (0.39 × 15 cm, Waters). Elution was achieved with a gradient of 20 to 70% of acetonitrile in 0.1% TFA for 23 min and monitored at 220 nm. H6 was eluted at the retention time of 20.2 min. The concentration of the remaining H6 was determined from the peak area, which was measured with a 807-IT integrator (Jasco).

RESULTS

Amino Acid Composition of H6—The amino acid composition of the purified enzyme is shown in Table I. The protein had a high content of acidic amino acids, cysteine, and glycine. This agrees well with its isoelectric point of 4.8 (*6*).

Sequence Analysis of H6—Digestion of CM-H6 with Lys-C and Arg-C gave several peptides (K1–K21 and R1–R9, respectively) after separation of the digest by reverse-phase HPLC (data not shown). Because peptide K7 was heterogeneous, it was further purified on the same column to yield two peptides, K7a and K7b. Since peptide K20 was too large to determine its whole sequence by the manual sequencing method, it was further digested with Asp-N to yield ten peptides (K13D1–K13D10) (data not shown). CM-H6 was also subjected to chemical cleavage at Met-X bonds with CNBr to give peptides M1–M13.

Edman degradation of peptides M12 and W4 liberated no amino acid. Because direct sequencing of the intact H6 and CM-H6 was also unsuccessful, the N-terminus of the protein might be blocked, probably by a pyroglutamyl residue. Therefore, the intact H6 and peptide M12 were sequenced after digestion with pyroglutamate aminopeptidase. In the

TABLE I. **Amino acid compositions of brevilysin H6 and its autoproteolytic fragments, p29K and the 45 kDa protein.**

Amino acid	H6		p29K	45 kDa protein	
	(A)*	(S)*	(S)	(A)	(S)
Asp	60.5	60	29	42.1	42
Thr	18.1	19	7	10.8	12
Ser	25.1	26	13	22.0	23
Glu	38.2	37	25	30.7	31
Pro	20.8	21	13	18.4	19
Gly	36.0	35	22	31.5	31
Ala	21.0	21	10	16.2	16
Cys	35.5	35	28	33.2	35
Val	22.8	25	10	14.4	16
Met	11.3	12	4	7.6	9
Ile	17.8	20	4	13.8	15
Leu	22.5	23	7	12.2	12
Tyr	22.5	23	12	16.3	18
Phe	10.4	10	4	8.4	8
His	15.5	15	6	12.9	13
Trp	2.4	4	1	1.2	2
Lys	22.9	23	14	15.3	15
Arg	9.6	10	3	3.8	4
Total		419	212		312

*A, data obtained on amino acid analysis; S, values calculated from the sequence.

case of peptide M10, no amino acid was detected at cycle 14. The presence of a following sequence, Cys(CM)-Ser, indicates that an *N*-linked sugar chain is attached to residue 14 (Asn-181) of this peptide. Because the information derived from the peptides described above is still insufficient to correlate the sequences of fragments, we used some peptides derived on V8 digestion and chemical cleavage at Trp-X bonds with *o*-iodosobenzoic acid. The amino acid compositions of all the peptides agreed well with the sequence (data not shown).

The arrangement of fragments along with the complete amino acid sequence of H6 is summarized in Fig. 1. The cleavage site of peptide K16 does not agree with the specificity of Lys-C. Since the sequence of K16 corresponds to the N-terminal part of p29K, this peptide may be derived through autoproteolysis of H6, as described below. The protein was composed of 419 amino acid residues amounting to 46,439 Da. Residues 208–419 of H6 were completely identical to the whole sequence of p29K (*7*), which comprised disintegrin-like and cysteine-rich domains.

Effect of Ca^{2+} on the Stability of H6—As we have already reported, calcium ions enhance the activity of H6 (*6*). The effects of Ca^{2+} on the stability of the enzyme as to pH, heating and urea were examined. In the absence of Ca^{2+}, the enzyme was most stable at pH 6.8 (Fig. 2A). The addition of calcium ions significantly stabilized the enzyme, and the full activity was maintained in the pH range of 5.6 to 8.5 (Fig. 2A). H6 was heated in 10 mM TES-NaOH (pH 7.0) at

Fig. 1. **Summary of amino acid sequence analysis of brevilysin H6.** Peptides derived from H6 on digestion with Lys-C (K), Arg-C (R), Asp-N (D), V8 protease (V), CNBr (M), or *o*-iodosobenzoic acid (W) are shown above the sequences. <E denotes 5-pyrrolidone-2-carboxylic acid. ♀ indicates a sugar chain linked to an asparagine residue. Arrowheads indicate the sites of autoproteolysis.

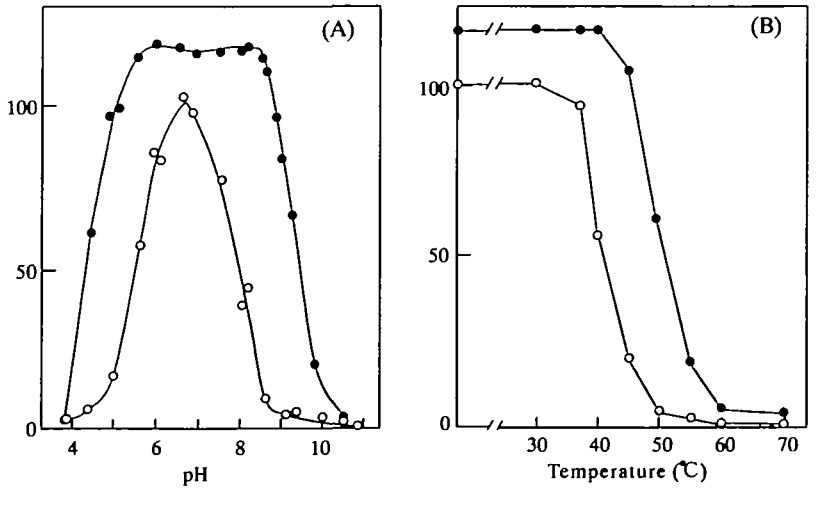

Fig. 2. **Stability of brevilysin H6.** (A) Stability at various pHs. H6 was pre-incubated in 50 mM veronal-HCl (pH 3.8–9.0) or 50 mM Gly-NaOH (pH 8–10.9) in the absence (○) or presence (●) of 2 mM $CaCl_2$ at 37°C for 1 h. (B) Thermal stability of H6. The protease was stood for 15 min at 0–70°C in 10 mM TES-NaOH (pH 7.0) in the absence (○) or presence (●) of 2 mM $CaCl_2$. The residual activity was measured in 0.2 M Tris-HCl (pH 8.5) at 37°C using casein as the substrate.

37–70°C for 15 min in the presence and absence of 2 mM $CaCl_2$, and then the residual activity was determined. The activity was markedly reduced above 40°C (Fig. 2B). The addition of Ca^{2+} ions increased the thermal stability by 10°C.

The caseinolytic activity of H6 dose-dependently decreased on the addition of urea (Fig. 3). However, the presence of 4 mM $CaCl_2$ significantly prevented this loss of enzyme activity. The activity of brevilysin L4 (*14*), a low molecular mass metalloprotease from the same venom, was also decreased by urea (Fig. 3). In contrast to H6, calcium ions did not affect the stability of brevilysin L4.

Cysteine is a strong inhibitor of H6 (*6*). We next determined the effect of Ca^{2+} on the inhibitory action of cysteine.

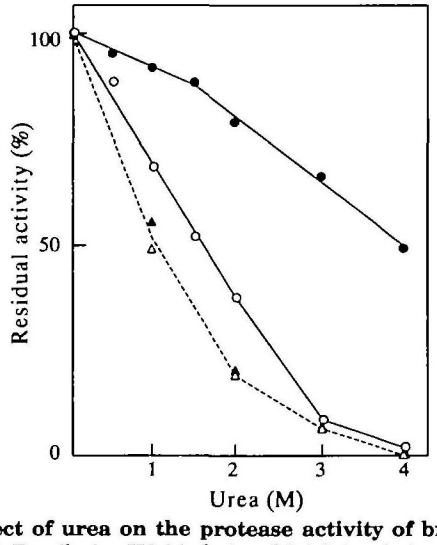

Fig. 3. **Effect of urea on the protease activity of brevilysins H6 and L4.** Brevilysins H6 (circles) and L4 (triangles) were pre-incubated in 50 mM TES-NaOH (pH 7.0) containing urea with (closed symbols) or without (open symbols) 4 mM $CaCl_2$ at 37°C for 5 min. The residual activity was measured in 0.2 M Tris-HCl (pH 8.5) at 37°C using FTC-casein as the substrate.

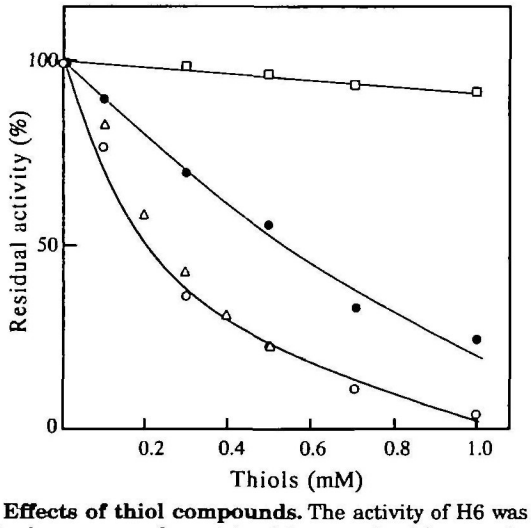

Fig. 4. **Effects of thiol compounds.** The activity of H6 was measured in the presence of L-cysteine (○), D-cysteine (△), L-cysteine plus 1 mM $CaCl_2$ (●), or the reduced form of glutathione (□) using 0.2% FTC-casein in 50 mM Tris-HCl (pH 8.5) at 37°C for 10 min.

As shown in Fig. 4, IC_{50} of L-cysteine was about 0.2 mM. Calcium ions markedly protected the enzyme activity, and IC_{50} increased to 0.5 mM. D-Cysteine was also effective. Another thiol compound, glutathione, had little effect (Fig. 4).

Autoproteolytic Digestion of H6—Autoproteolysis of many P-III type metalloproteases takes place, which yields a large fragment with a molecular mass of 29–34 kDa (*15*, *16*). However, the peptide bonds that are split during this autoproteolysis have not yet been determined in detail. Since H6 also undergoes such autoproteolysis (*7*), we examined the effects of Ca^{2+} and cysteine on the autoproteolysis of H6. The rate of autoproteolysis was dependent on pH and maximal at the optimum pH of the enzyme (data not shown). The reaction was rapid at pH 8.5 in the absence of Ca^{2+}, and obeyed first-order kinetics (Fig. 5). The first-order rate constant (k_1) was calculated to be 0.0145 min^{-1} at 37°C

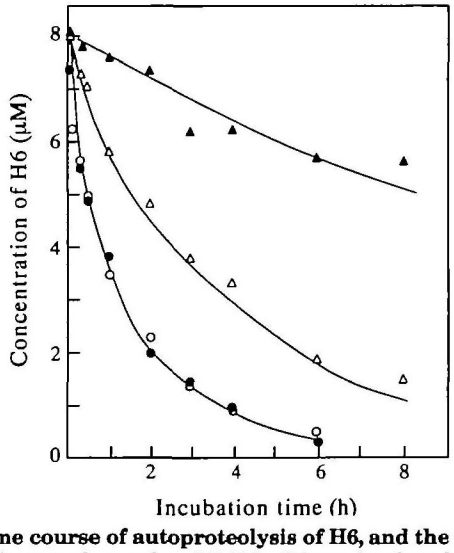

Fig. 5. **Time course of autoproteolysis of H6, and the effects of calcium ions and cysteine.** H6 (0.8 μM) was incubated at 37°C in 50 mM Tris-HCl (pH 8.5) in the absence (○) or presence of 0.1 mM cysteine (●), 1 mM $CaCl_2$ (△), or 10 mM $CaCl_2$ (▲). After the reaction had been stopped with EDTA, aliquots were subjected to HPLC on a μBondasphere C8-300A column (0.39 × 15 cm), and then the concentration of the remaining H6 was determined.

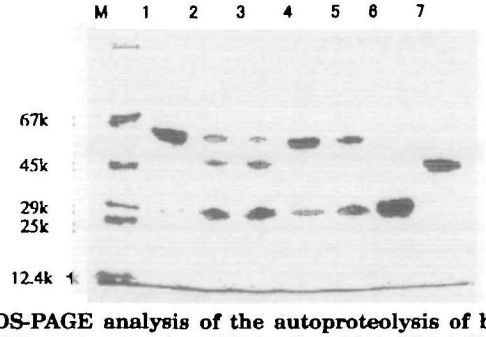

Fig. 6. **SDS-PAGE analysis of the autoproteolysis of brevilysin H6.** H6 was incubated at 37°C in 50 mM Tris-HCl (pH 8.5) in the absence of $CaCl_2$ for 6 h (lane 2) and 24 h (lane 3), or in the presence of 10 mM $CaCl_2$ for 6 h (lane 4) and 24 h (lane 5). Lanes 1, 6, and 7 are the purified H6, p29K and 45 kDa protein, respectively. M, marker proteins: bovine serum albumin, ovalbumin, carbonic anhydrase, chymotrypsinogen, and cytochrome *c* (from top to bottom).

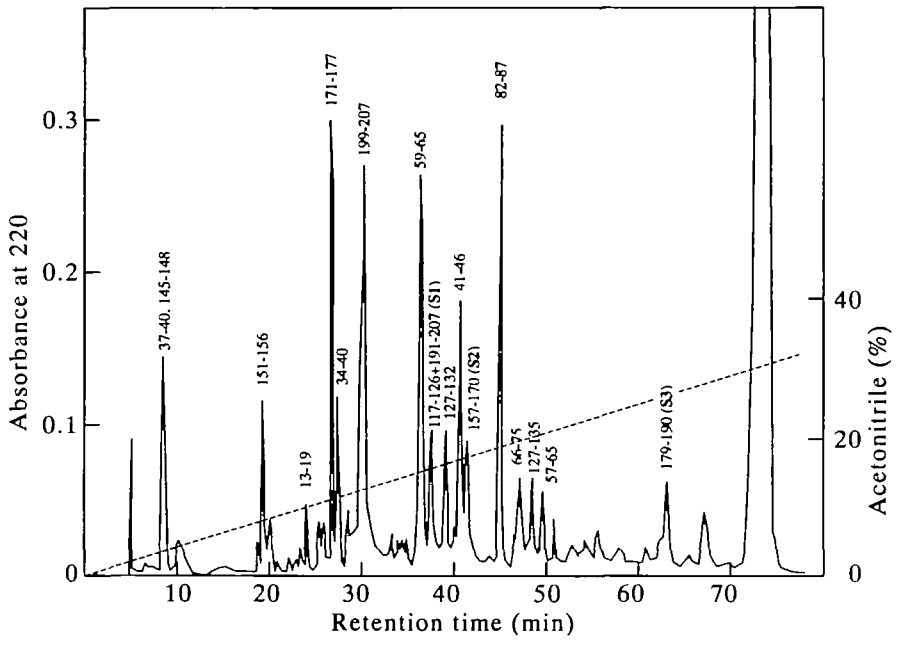

Fig. 7. **Separation of fragment peptides derived from the autoproteolytic digest of H6.** After the intact H6 had been incubated in 50 mM Tris-HCl (pH 8.5) at 37°C for 60 h, the reaction mixture was applied to a Biofine RPC SC-18 column (0.46 × 25 cm). The numbers above the peaks are the corresponding residues in the sequence of H6. Cystine-containing peaks are designated as S1–S3.

and pH 8.5. The addition of an inhibitory concentration of cysteine (0.1 mM) had no effect on the autoproteolysis (k_1 = 0.0147). On the contrary, calcium ions significantly suppressed the reaction. The k_1 values were calculated to be 0.0046 and 0.0007 min^{-1} for 1 and 10 mM Ca^{2+}, respectively.

Autoproteolysis of H6 was also followed by SDS-PAGE (Fig. 6). In the absence of Ca^{2+}, two new bands of 29 and 45 kDa were observed. On the other hand, the 45-kDa band was not detected in the presence of 10 mM Ca^{2+} ions.

The 29 and 45 kDa proteins were purified from a 24-h autodigest of H6 by ion-exchange HPLC on a DEAE column (data not shown). Both proteins showed no proteolytic activity but retained the inhibitory activity as to the aggregation of platelets. The amino acid composition of the 45 kDa protein is shown in Table I. Direct sequencing of the 29 kDa protein yielded the sequence of IVSPPVXGNE, which corresponds to the N-terminus of p29K. The 45 kDa protein had the sequence of LTAIDFNGPT, which corresponds to residues 99–108 of H6. Thus, the Leu^{98}-Leu^{99} and Asp^{207}-Ile^{208} bonds were proved to be the most susceptible as to the autoproteolysis of H6.

When the intact H6 was incubated at 37°C for 60 h, several peptide fragments were generated, as shown by reverse phase HPLC (Fig. 7). The locations of these fragments along the primary structure of H6, which has determined by amino acid and sequence analyses, are also presented in Fig. 7. The last peak was identified as p29K on SDS-PAGE. The sites in H6 split on autoproteolysis are indicated by arrowheads in Fig. 1. More than twenty-five bonds were cleaved. The amino sides of the peptide bonds adjacent to hydrophobic residues such as Ile, Leu, Val, Met, Phe, and Tyr were preferentially attacked by the enzyme itself.

Location of Disulfide Bridges in H6—H6 has a free SH group (*6*), while no free cysteine residue was found in p29K (*7*). Furthermore, no disulfide bond linked p29K and the rest of H6 molecule. The amino acid composition of a cystine-containing peptide (S1) in Fig. 7 corresponded to the sum of residues 117–126 and 191–207. S3 was estimated to be derived from residues 179–190 by amino acid analysis. The sequences of these peptides were also confirmed by Edman degradation, that is,

S1, M-X-H-P-K-R-S-V-G-I
I-M-D-H-N-P-E-X-I-V-N-E-P-L-G-T-D

S3, F-S-X-X-S-Y-I-Q-X-W-D-F

The results indicated that two disulfide bonds link Cys-118 to Cys-198 and Cys-182 to Cys-187. Another disulfide bond was assumed to be present between Cys-165 and Cys-158 or 160, thus indicating that Cys-158 or 160 is a free cysteinyl residue. Sequencing of Cys-containing peptide S2 gave no clear result.

DISCUSSION

The sequence of H6 was established by manual Edman degradation of overlapping peptides generated with a variety of selective cleavage procedures. H6 consists of 419 amino acids and its calculated M_r is 46,439. The difference between this value and the apparent M_r (60,000) determined on SDS-PAGE would be due to the presence of a carbohydrate chain at Asn-181 and the tight conformation due to the high content of disulfide bridges. The latter suppress the binding of SDS molecules to proteins and retard their migration in a gel.

The amino acid sequence of H6 was compared with those of venom metalloproteases (Fig. 8). H6 is a P-III class protein possessing a three domain structure: metalloprotease (residues 1–203), disintegrin-like (residues 204–296), and cysteine-rich (residues 297–419) domains. The cysteine residues of H6 are highly conserved in each domain. A conservative zinc-chelating sequence of reprolysins (HEXXHXXGXXH) (*21*) is located at residues 143–153. H6 showed the highest similarity to jararhagin (*18*), a metalloprotease

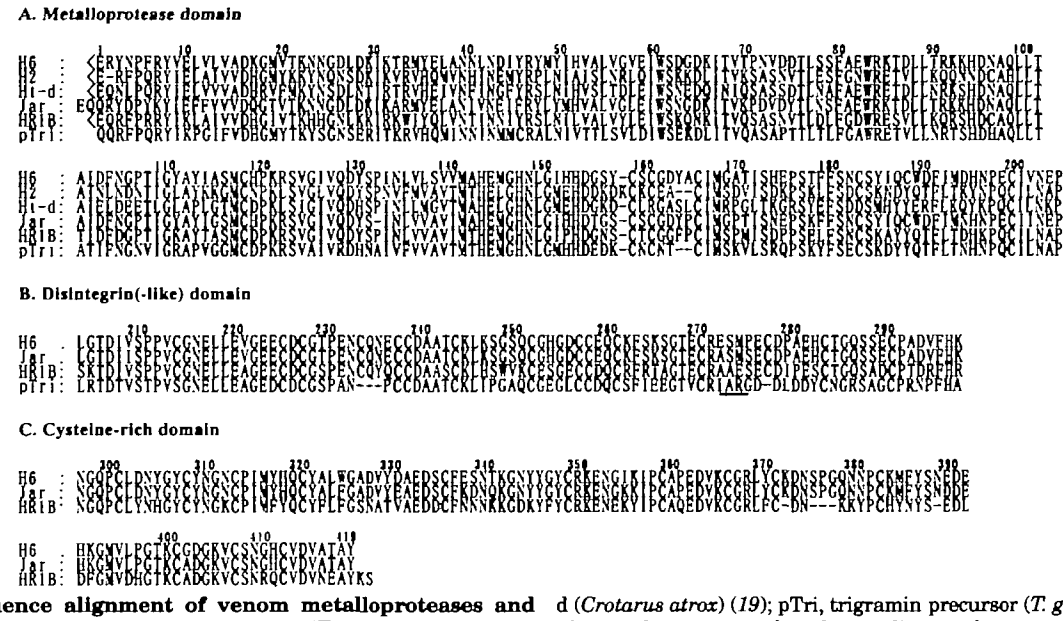

Fig. 8. **Sequence alignment of venom metalloproteases and disintegrin precursors.** H2, H_2-proteinase (*Trimeresurus flavoviridis*) (*17*); Jar, jararhagin (*Bothrops Jararaca*) (*18*); HR1B, hemorrhagic factor HR1B (*T. flavoviridis*) (*2*); Ht-d, hemorrhagic factor Ht-d (*Crotarus atrox*) (*19*); pTri, trigramin precursor (*T. gramineus*) (*20*). The residues are numbered according to the sequence of H6. The RGD sequence of trigramin is underlined.

from *Bothrops jararaca* venom (88.3% identity).

The metalloprotease domain of H6 also showed high similarity to P-I class metalloproteases (Fig. 8). Although many venom metalloproteases exhibit hemorrhagic activity, some P-I class proteases such as brevilysins L4 (*14*), H_2-proteinase (*17*), fibrolase (*22*), and adamalysin II (*23*) are non-hemorrhagic. However, there seems to be no obvious characteristic of hemorrhagic and non-hemorrhagic proteases with respect to the sequences in their metalloprotease domains. The hemorrhagic activity of H6 is related to its proteinase activity since the removal of Zn^{2+} ions with EDTA abolished both activities, and the thermal stability of the protease activity correlated well with the hemorrhagic activity (data not shown).

P-III class metalloproteases are autocatalytically degraded to give a fragment with a molecular mass of about 30 kDa (*15*, *16*). H6 also loses the proteolytic activity during incubation at the optimum pH through autoproteolysis (*7*). Hence, its protease activity cannot be used to evaluate the rate of autoproteolysis. Instead, we directly measured the remaining H6 by HPLC. In the absence of Ca^{2+}, H6 rapidly produced two large fragments (p29K and a 45 kDa protein), which corresponded to residues 208–419 and 99–419 of H6, respectively. This indicates that the autoproteolysis was initiated by splitting at either the Leu^{98}-Leu^{99} or Asp^{207}-Ile^{208} bond. The half-life of H6 was 48 min at 37°C and pH 8.5 in the absence of Ca^{2+}. According to Takeya *et al.* (*16*), the half-life for the proteolytic activity of HR1A was about 5.5 h, and the degradation was completely suppressed by 10 mM Ca^{2+}.

On the other hand, the presence of 10 mM Ca^{2+} increased the half-life of H6 to about 16.5 h. Furthermore, Ca^{2+} significantly suppressed the formation of the 45 kDa protein (Fig. 6). The Leu-98 and Leu-99 residues are located in the C-terminal part of β-strand III, and a long loop starts at the ends of these residues in adamalysin II (*23*) and H_2-proteinase (*24*). If the metalloprotease domain of H6 has a similar conformation to these proteinases, protection against cleavage at the Leu^{98}-Leu^{99} bond by Ca^{2+} may suggest that the ion binds to the loop near these residues and thereby stabilizes the tertiary structure.

Scissile peptide bonds are widely distributed in the metalloprotease domain (Fig. 1). Venomous metalloproteases generally cleave peptides and proteins on the amino side of peptide bonds adjacent to hydrophobic residues (*25*). All the peptide bonds split on autoproteolysis met this rule, as shown in Fig. 1. The peptide bond inside the disintegrin and cysteine-rich domains was not split even after 60 h. It is noteworthy that p29K resisted the proteolytic attack by trypsin, chymotrypsin and *S. aureus* V8 protease. This suggests that the C-terminal half of the H6 molecule has a tight conformation due to many disulfide bridges.

Jararhagin-C, a 28-kDa fragment of jararhagin, was reported to inhibit platelet aggregation (*15*). Only ten residues are different in the sequences of jararhagin-C and p29K (95% identity). H6 and p29k also inhibit human platelet aggregation (*7*). That H6 exhibits strong α-fibrinogenolytic activity (*6*) may partly be explained by rapid consumption of fibrinogen in platelet-rich plasma. However, Jia *et al.* (*26*) reported that the platelet inhibitory activity of atrolysin A, a hemorrhagic metalloprotease from *C. atrox*, is attributable to its disintegrin-like/cysteine-rich domain. Moreover, they proved, using synthetic peptides, that two acidic residues in the RSECD sequence, in lieu of the disintegrin signature sequence (RGD), are essential for the inhibition of platelet aggregation, and that the cysteinyl residue must be constrained by participation in a disulfide bond with another cysteinyl residue. The MPECD sequence at residues 273–277 in H6 may participate in the disintegrin-like activity.

REFERENCES

1. Rawlings, N.D. and Barrett, A.J. (1995) Evolutionary families of metallopeptidases in *Methods in Enzymology* (Barrett, A.J., ed.) Vol. 248, pp. 183–228, Academic Press, New York
2. Takeya, H., Oda, K., Miyata, T., Omori-Satoh, T., and Iwanaga, S. (1990) The complete amino acid sequence of the high molecular mass hemorrhagic protein HR1B isolated from the venom of *Trimeresurus flavoviridis*. *J. Biol. Chem.* **265**, 16068–16073
3. Hite, L.A., Jia, L.G., Bjarnason, J.B., and Fox, J.W. (1994) cDNA sequences for four snake venom metalloproteinases: structure, classification, and their relationship to mammalian reproductive proteins. *Arch. Biochem. Biophys.* **308**, 182–191
4. Blobel, C.P., Wolfsberg, T.G., Turck, C.W., Myles, D.G., Primakoff, P., and White, J.M. (1992) A potential fusion peptide and an integrin ligand domain in a protein active in sperm-egg fusion. *Nature* **356**, 248–252
5. Perry, A.C.F., Jones, R., Barker, P.J., and Hall, L. (1992) A mammalian epididymal protein with remarkable sequence similarity to snake venom haemorrhagic peptides. *Biochem. J.* **286**, 671–675
6. Terada, S., Kimoto, E., Kawasaki, H., Hao, W.-X., and Li, H.-W. (1991) Purification of a metalloprotease from Chinese Mamushi (*Agkistrodon halys brevicaudus*) venom. *Fukuoka Univ. Sci. Rep.* **21**, 147–153
7. Terada, S., Hirakawa, Y., and Fujimura, S. (1998) Primary structure of a 29 kDa-protein with platelet inhibitory activity isolated from the venom of *Agkistrodon halys brevicaudus*. *Fukuoka Univ. Sci. Rep.* **28**, 99–109
8. Twining, S.S. (1984) Fluorescein isothiocyanate-labeled casein assay for proteolytic enzymes. *Anal. Biochem.* **143**, 30–34
9. Laemmli, U.K. (1970) Cleavage of structural proteins during the assembly of the head of bacteriophage T4. *Nature* **227**, 680–685
10. Hirs, C.H.W. (1967) Reduction and *S*-carboxymethylation of proteins in *Methods in Enzymology* (Hirs, C.H.W., ed.) Vol. 11, pp. 199–203, Academic Press, New York
11. Chang, T.-Y. (1979) Manual solid phase sequence analysis of polypeptides using 4-*N*,*N*-dimethylaminoazobenzene 4′-isothiocyanate. *Biochim. Biophys. Acta* **578**, 188–195
12. Terada, S., Fujimura, S., Noda, K., and Kimoto, E. (1992) Separation of dimethylaminoazobenzenethiohydantoin derivatives by a reversed-phase high-performance liquid chromatography. *Fukuoka Univ. Sci. Rep.* **22**, 35–39
13. Satake, M., Murata, Y., and Suzuki, T. (1963) Studies on snake venoms. XIII. Chromatographic separation and properties of three proteinases from *Agkistrodon halys blomhoffii* venom. *J. Biochem.* **53**, 438–447
14. Fujimura, S., Rikimaru, T., Baba, S., Hori, J., Hao, X.Q., Terada, S., and Kimoto, E. (1995) Purification and characterization of a non-hemorrhagic metalloprotease from *Agkistrodon halys brevicaudus* venom. *Biochim. Biophys. Acta* **1243**, 94–100
15. Usami, Y., Fujimura, Y., Miura, S., Shima, H., Yoshida, E., Yoshioka, A., Hirano, K., Suzuki, M., and Titani, K. (1994) A 28 kDa-protein with disintegrin-like structure (jararhagin-C) purified from *Bothrops jararaca* venom inhibits collagen- and ADP-induced platelet aggregation. *Biochem. Biophys. Res. Commun.* **201**, 331–339
16. Takeya, H., Nishida, S., Nishino, N., Makinose, Y., Omori-Satoh, T., Nikai, T., Sugihara, H., and Iwanaga, S. (1993) Primary structures of platelet aggregation inhibitors (disintegrins) autoproteolytically released from snake venom hemorrhagic metalloproteinases and new fluorogenic peptide substrates for these enzymes. *J. Biochem.* **113**, 473–483
17. Takeya, H., Arakawa, M., Iwanaga, S., and Omori-Satoh, T. (1989) Primary structure of H_2-proteinase, a non-hemorrhagic metalloproteinase, isolated from the venom of the Habu snake, *Trimeresurus flavoviridis*. *J. Biochem.* **106**, 151–157
18. Paine, M.J.I., Desmond, H.P., Theakston, R.D.G., and Crampton, J.M. (1992) Purification, cloning, and molecular characterization of a high molecular weight hemorrhagic metalloprotease, jararhagin, from *Bothrops jararaca* venom. *J. Biol. Chem.* **267**, 22869–22876
19. Shannon, J.D., Baramova, E.N., Bjarnason, J.B., and Fox, J.W. (1989) Amino acid sequence of a *Crotalus atrox* venom metalloproteinase which cleaves type IV collagen and gelatin. *J. Biol. Chem.* **264**, 11575–11583
20. Neeper, M.P. and Jacobson, M.A. (1990) Sequence of a cDNA encoding the platelet aggregation inhibitor trigramin. *Nucleic Acids Res.* **18**, 4255
21. Murphy, G.J.P., Murphy, G., and Reynolds, J.J. (1991) The origin of matrix metalloproteinases and their familiar relationship. *FEBS Lett.* **289**, 4–7
22. Randolph, A., Chamverlain, S.H., Chu, H.-L.C., Retzios, A.D., Markland, F.S., Jr., and Masiarz, F.R. (1992) Amino acid sequence of fibrolase, a direct-acting fibrinolytic enzyme from *Agkistrodon contortrix contortrix* venom. *Protein Sci.* **1**, 590–600
23. Gomis-Rüth, F.X., Kress, L.F., Kellermann, J., Mayr, I., Lee, X., Huber, R., and Bode, W. (1994) Refined 2.0 Å X-ray crystal structure of the snake venom zinc-endopeptidase adamalysin II. *J. Mol. Biol.* **239**, 513–544
24. Kumasaka, T., Yamamoto, M., Moriyama, H., Tanaka, N., Sato, M., Katsube, Y., Yamakawa, Y., Omori-Satoh, T., Iwanaga, S., and Ueki, T. (1996) Crystal structure of H_2-proteinase from the venom of *Trimeresurus flavoviridis*. *J. Biochem.* **119**, 49–57
25. Yamakawa, Y., Omori-Satoh, T., and Sadahiro, S. (1987) Purification, characterization and substrate specificity of a basic proteinase in the venom of Habu (*Trimeresurus flavoviridis*). *Biochim. Biophys. Acta* **925**, 124–132
26. Jia, L.-G., Wang, X.-M., Shannon, J.D., Bjarnason, J.B., and Fox, J.W. (1997) Function of disintegrin-like/cysteine-rich domains of atrolysin A. Inhibition of platelet aggregation by recombinant protein and peptide antagonists. *J. Biol. Chem.* **272**, 13094–13102